CHAPTER VI *PLASTIC DEFORMATION:*
Introduction to the dislocation model

6.1 Phenomenology of plastic deformation

For most engineering cases and realistic scenarios, the deformation of solids is a combination of plastic and elastic deformation. For example, plastic deformation in rolled metal sheets can be as large as 80%. At such large deformations, some residual elastic deformations still exist from internal stresses of defects introduced in the crystal lattice during the rolling process. We have introduced the elastic deformation theory in Chapter III. Here, we discuss plastic deformation, which is not a simple extension of the Landau-Lifshitz elasticity theory to higher strains. Thus, to accurately describe plastic deformation, we must introduce the structural elements of materials that are typically neglected in the study of elastic properties. This Chapter aims to illustrate plastic deformation, starting with the dislocation model, even though these are not the only "sources" of plastic deformation.

6.1.1 Experimental observations

After plastic deformation, the surface of monocrystalline samples often shows characteristic lines (Figure 6-1). Plastic deformation is produced due to the "sliding" part of the solid (Figure 6-2) while maintaining the prior crystallographic orientation.

For most cases, the surface separating the two parts, which shifts, is generated by a straight line parallel to the surface, resulting in a plane known as a "glide plane." The lines formed by the intersection of the glide planes and the sample surface are referred to as "slip" or "glide lines."

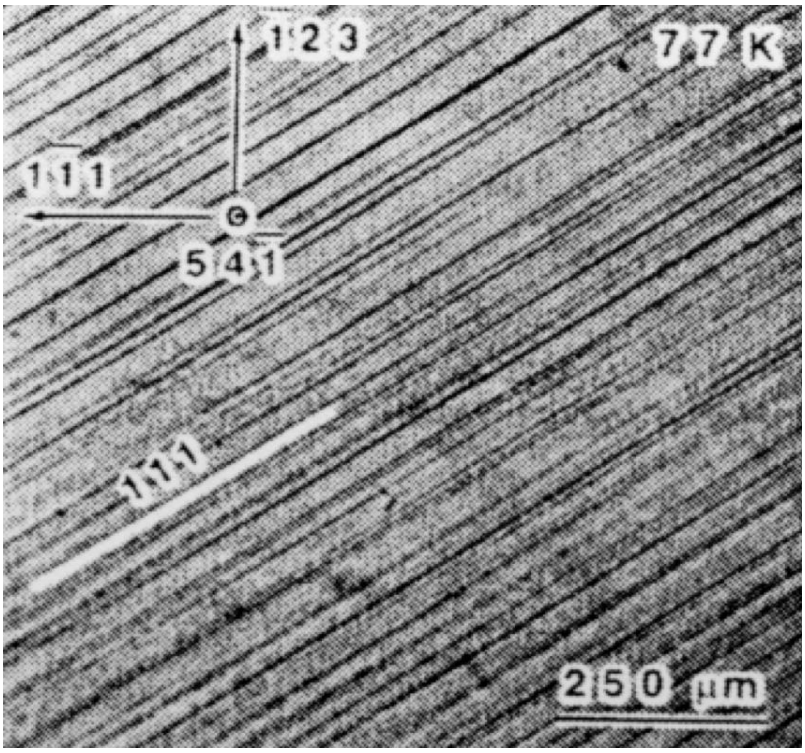

Figure 6-1: *Monocrystal of Ni_3Al deformed at T=77K*

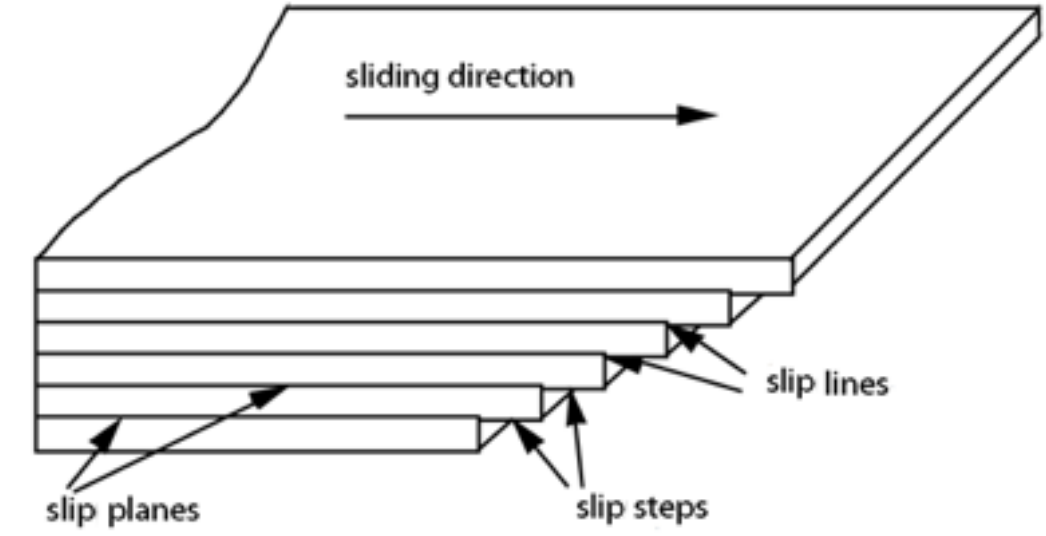

Figure 6-2: *Diagram of the surface of the sample in Figure 6-1*

From experimental observations, we note here that:

- The "sliding" is not the only mode of plastic deformation, but it is very often the most important one,
- Even though an elongation is produced, plastic deformation acts by shear deformation along characteristic planes of the crystal,
- The previously mentioned glide lines indicate that plastic deformation is heterogeneous and concentrated in certain glide planes. The regions between the slip step surfaces are untouched by the deformation.

6.1.2 Relations between sliding and crystal structure

Early researchers over a century ago had difficulty envisioning the Relation between plastic deformation and the atomic structure of crystals due to the lack of advanced imaging techniques, e.g., high-resolution TEM, controlled materials processing, and other experimental methods. In 1912, when Max von Laue demonstrated the crystalline nature of metals, a new approach was required. Metals have relatively simple crystal structures: FCC [Au, Al, Ag, Cu, ...], HCP [Zn, Mg, ...], BCC [Fe, W, Mo, Nb, Ta, ...]. Therefore, it was preferable to manufacture single-phase monocrystals to study plastic deformation mechanisms that are less complex than those in polycrystalline samples. As a result, we can observe strain-stress curves of the kind shown in Figures 6-3. In most cases, we observe that a first domain (stage I) exists where plastic deformation occurs readily, and the monocrystal deforms as a "stack of cards," i.e., by shear along the glide planes.

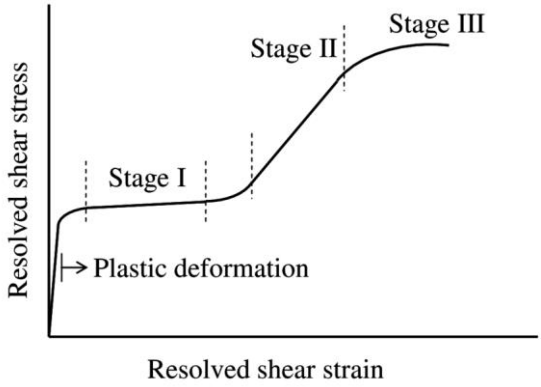

Figure 6-3: *After the first phase of easy" deformation (stage I), we generally observe hardening to the extent that the deformation has linear, elastic behavior(stage II). This hardening can be followed by another deformation phase (stage III), characterized by the activation of other gliding mechanisms on less dense atomic planes. The curves a) and b) refer to tensile and compressive deformation, respectively.*

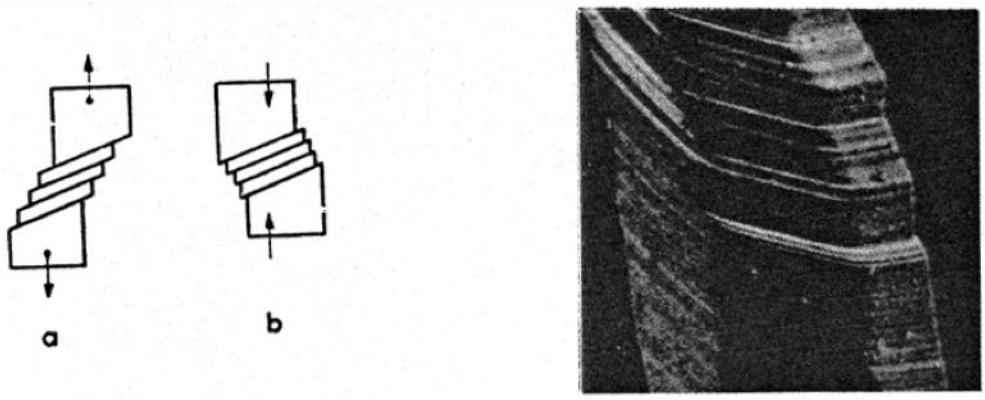

Figure 6-4: *Step" edges appearing on the surface of a deformed monocrystal*

The observation of the glide lines enables us to determine the glide planes; in FCC and HCP metals, these are, in general, highly dense planes [(111) for FCC, (0001) for HCP]. Moreover, the direction of the deformation is almost always in a dense direction ([110] in FCC, [110] in HCP, and [111] in CC). Thus, plastic deformation typically manifests as a shear deformation.

Schmid and Boas have determined that gliding always occurs when the shear stress τ, for a glide plane and direction, reaches a characteristic threshold $\tau = \tau c$, which is dependent on the nature of the crystal but independent of the orientation of the stress axis to the crystal lattice. If the axis of traction forms an angle λ with the glide direction and an angle Φ with the glide plane, the force component in

$$\tau = \frac{F}{S}\cos\Phi cos\lambda = \sigma cos\Phi cos\lambda \qquad (6.1)$$

the direction of the sliding is $Fcos\lambda$, while the area of the glide plane is $S/cos\Phi$, or τ is called the projected stress, and $m=cos\Phi cos\lambda$ is the Schmid factor. Therefore, when multiple glide systems exist (a glide system is defined by a glide plane and direction), τ reaches the threshold τ_c for at least one of the possible crystallographic systems if the stress σ is progressively increased. Thus, the first glide system that activates has the highest Schmid factor and shear stresses that trigger plastic deformation.

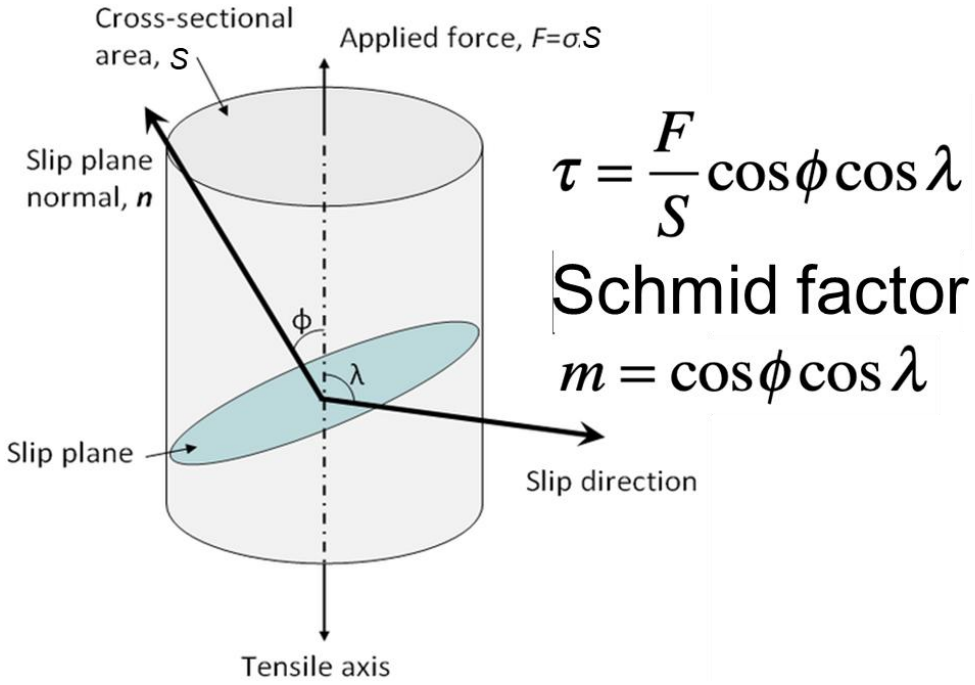

Figure 6-5: *Definition of the angles Φ and λ in the Schmid factor*

6.2 Elastic yield strength and the dislocation concept

6.2.1 Rigid gliding over a plane

The simplest hypothesis to explain previous observations is that the atomic movements between planes are rigid and coherent, i.e., all the atoms in a plane move simultaneously and in coordination. If the top part of the crystal slides rigidly over the bottom part (Figure 6-6a), we expect the stress σ to be periodic (Figure 6-6b):

- periodic with a period b,
- symmetrical to displacement,
- zero for stable equilibrium (*x=0*) and unstable (*x=b/2*).

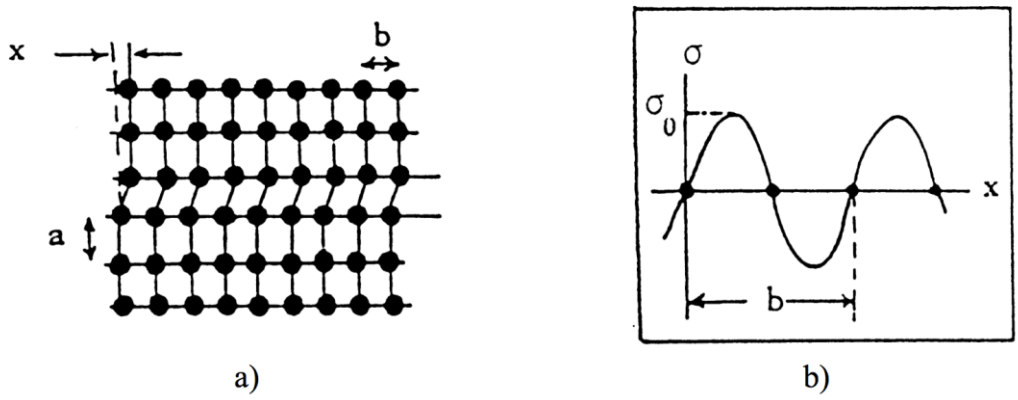

Figure 6-6: *Rigid gliding hypothesis, a plane moving over a plane*

The simplest solution for this periodic stress is given by:

$$\sigma = \sigma_0 sin\left(\frac{2\pi x}{b}\right) \tag{6.2}$$

The constant σ_0 can be estimated to a first approximation starting from the linear elasticity for small displacements (small x), where there is a direct proportionality between the stresses and the shear (cf Chapter III), i.e.,

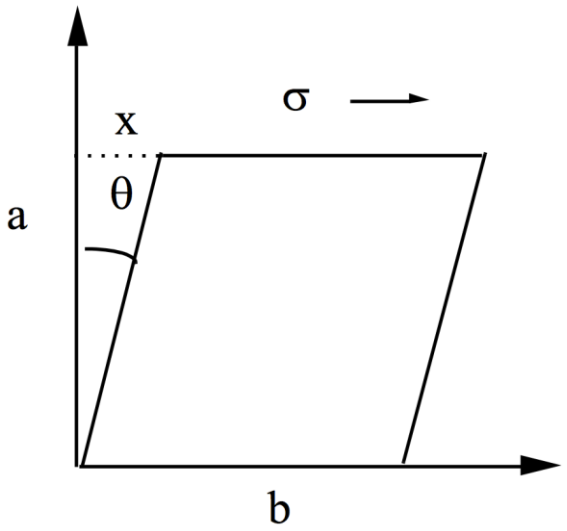

Figure 6-7 : *Simple Shear*

$$\sigma = \mu\theta = \mu\frac{x}{a} \cong \sigma_0\frac{2\pi x}{b}$$

where μ is the shear modulus, so that:

$$\sigma_0 = \frac{\mu}{2\pi}\frac{b}{a}$$

from which we can write:

$$\sigma = \frac{\mu}{2\pi}\frac{b}{a}\sin\frac{2\pi x}{b}$$

The maximum value of this expression in x = b/4 gives the value of the theoretical elastic yield strength:

$$\sigma_{th} = \frac{\mu}{2\pi}\frac{b}{a} \approx \frac{\mu}{10}$$

The value of μ/10, referred to as the theoretical Frenkel limit, does not align with experimental evidence; instead, we find values for the yield limit in the order of magnitude of μ.

For example, for copper:

μ ≈ 45 GPa or $\sigma_{th} \approx 4500$ MPa. Experimentally, σ_{ys} is in the order of a few MPa.

6.2.2 Localized gliding

a) Occurrence of local plastic deformations

The amount of deformation can be obtained by measuring, for example, the relative displacements of the faces of an elementary cube between the initial and final states. The plastic deformation of the elementary cube is obtained without applied stress. For this purpose, the cube is partitioned into layers perpendicular to the direction x_j with a thickness ∂x_j. We give the relative displacement between two consecutive layers ∂u_i and take the limit for $\partial x_j \to 0$ while keeping the ratio constant $\partial u_i / \partial x_j$. If some gaps appear (Figure 6-8c), these are filled with external matter until the local density is again homogeneous. The volume element is thus deformed in both a plastic and homogeneous way, remaining free of any stresses.

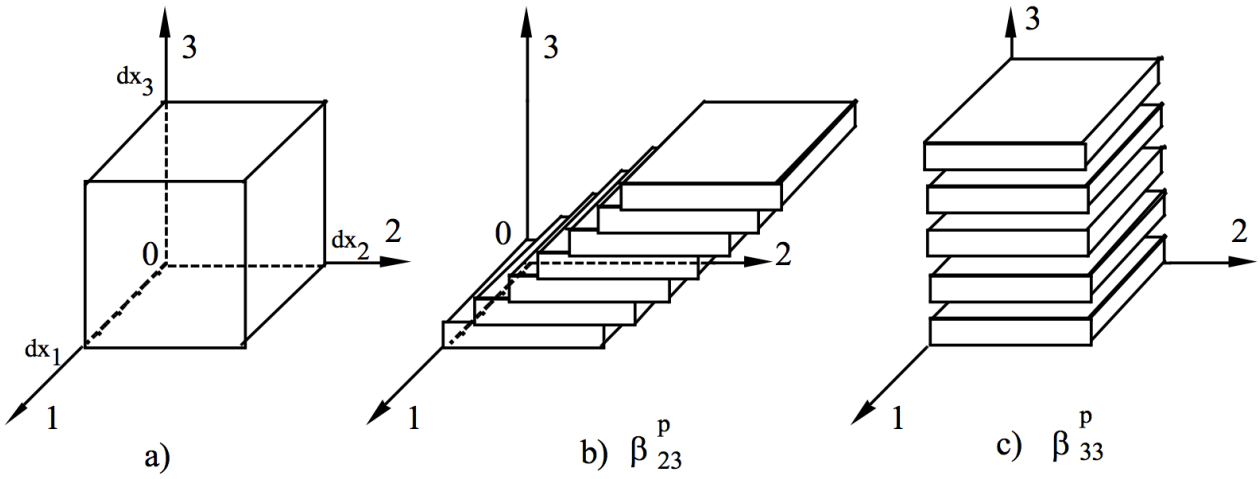

Figure 6-8: Realization of plastic deformations

Let du_i^p be the relative displacement in the direction *i* of the faces with orientation *j,* which limits the volume:

$$du_i^p = \int_0^{dx_j} \left(\frac{\partial u_i}{\partial x_j} \right) \partial x_j = \left(\frac{\partial u_i}{\partial x_j} \right) dx_j$$

As in the elastic case, letting $\beta_{ij}^p = \frac{\partial u_i}{\partial x_j}$, we have:

$$du_i^p = \beta_{ij} dx_j$$

where dx_j represents the separation in the initial configuration of the displaced faces. If the displacements occur on the three faces, then

$$du_i^p = \beta_{i1}^p dx_1 + \beta_{i2}^p dx_2 + \beta_{i3}^p dx_3$$

where du_i^p represents the projection on the axis *i* of the displacement vector $d\vec{u}$ of point (dx_1, dx_2, dx_3)to point O. We define thus the plastic displacement gradient tensor $\overline{\overline{\beta^p}}$ as:

$$\overrightarrow{du^p} = \overline{\overline{\beta^p}} d\vec{x} \tag{6.3}$$

Remark:

In the elastic case, the displacements are obtained by applying the stresses on the faces of the cube, though the definition of the elastic displacement gradient tensor $\overline{\overline{\beta^e}}$ is analogous to the formula (3.15):

$$\overrightarrow{du^e} = \overline{\overline{\beta^e}} d\vec{x}$$

The total deformation is:

$$d\vec{u} = d\overrightarrow{u^p} + d\overrightarrow{u^e} \tag{6.4}$$

We can then also write:

$$d\vec{u} = \bar{\bar{\beta}} d\vec{x} \text{ with } \bar{\bar{\beta}} = \overline{\overline{\beta^e}} + \overline{\overline{\beta^p}}$$

b) Compatibility conditions at the scale of the deformed body

The previous descriptions only consider deformation over an elementary cube without considering compatibility with the rest of the deformed body. To understand how the local deformations can comply with this continuity condition, let us cut the solid into elementary cubes and apply a plastic displacement gradient β^P dependent on the position of the solid. The cubes are free from any bounds during this operation, and their physical state is unaltered. When we try to rebuild the solid body, two cases arise:

i) The cubes adjust without gaps and stresses, and we obtain the same overall state of the deformed body.

ii) The cubes cannot be adjusted together (see Figure 6-9). It is necessary to have rotations and elastic deformations to maintain continuity and prevent gaps and cracks, which implies the presence of stresses within the body. After the solid has been reconstructed, we take away the applied forces. We then obtain the same final state that would have been there without the solid partition (for the same distribution of plastic displacement gradient β^P). Still, local stresses persist (internal stresses) distributed to minimize the corresponding elastic energy.

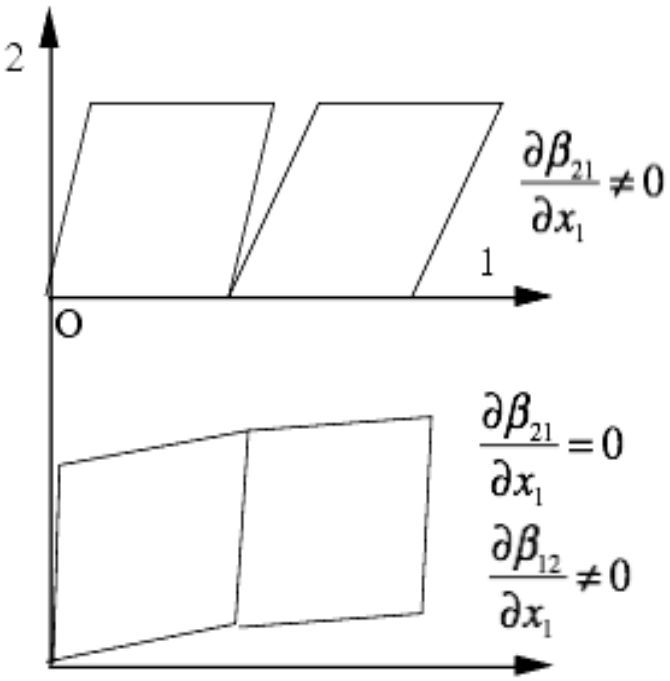

We want to express that the solid remains compact, i.e., with no cracks. This implies that the common face between two consecutive elements shares the same displacement. That is, for a common face in Figure 6-9, the components β_{12} are identical in O and in dx_1, that is to say,

$$\frac{\partial \beta_{21}}{\partial x_1} = 0$$

whereas β_{12} can vary in any way (Figure 6-9). That is, it must be:

$$\beta_{21,1} = \beta_{31,1} = 0$$

We can express it in a more general form by the following equation,

$$d\vec{u} = \frac{\partial \vec{u}}{\partial x_j} dx_j = \overrightarrow{\beta_j} dx_j$$

which is an exact differential.

Figure 6-9: *Plastic Deformation without adjustment*

This implies Cauchy's conditions:

$$\frac{\partial \overrightarrow{\beta_j}}{\partial x_k} = \frac{\partial \overrightarrow{\beta_k}}{\partial x_j} \text{ if } j \neq k$$

We can summarize these conditions in a more elegant form. For example, writing all the conditions, we have:

$$\begin{bmatrix} \frac{\partial \overrightarrow{\beta_3}}{\partial x_2} - \frac{\partial \overrightarrow{\beta_2}}{\partial x_3} \\ \frac{\partial \overrightarrow{\beta_1}}{\partial x_3} - \frac{\partial \overrightarrow{\beta_3}}{\partial x_1} \\ \frac{\partial \overrightarrow{\beta_2}}{\partial x_1} - \frac{\partial \overrightarrow{\beta_1}}{\partial x_2} \end{bmatrix} = 0 = \overrightarrow{rot}\,\overline{\overline{\beta}}$$

That is to say $\overrightarrow{rot}\,\overline{\overline{\beta^e}} = -\overrightarrow{rot}\,\overline{\overline{\beta^p}} = \overline{\overline{\alpha}}$

In fact, $\overrightarrow{rot}\,\overline{\overline{\beta}} \neq 0$ describes the distribution of "cracks" in the solid. The following shows that the tensor $\overline{\overline{\alpha}} = \nabla \wedge \overline{\overline{\beta^e}}$ is a source for the internal stress field.

c) Incompatible elasticity (internal stresses)

In the non-plastic case or else in the case of a plastic deformation that does not destroy the connection of the solid, $\overrightarrow{rot}\,\overline{\overline{\beta^p}} = 0$ and the previous condition ($\overrightarrow{rot}\,\overline{\overline{\beta^p}} = 0$) becomes,

$$\overrightarrow{rot}\,\overline{\overline{\beta^e}} = \nabla \wedge \overline{\overline{\beta^e}} = 0$$

which defines the classic theory of elasticity. This case only includes external forces applied to the surface of the body that result in pure elastic deformations, as no gaps occur, i.e., it satisfies the compatibility conditions.
In the general case, the plastic displacement gradient does not satisfy. Therefore, it is necessary that in the solid, elastic deformation exists such that $\nabla \wedge \overline{\overline{\beta^e}} = -\nabla \wedge \overline{\overline{\beta^p}}$ to reconstitute the connection within the solid. These induced elastic deformations correspond - via Hooke's law - to the existence of elastic stresses or "internal stresses," meaning that these exist within the solid even if no external force is applied on the external faces of the solid.

The equation then defines these internal stresses:

$$\overline{\overline{\alpha}} = \overrightarrow{rot}\,\overline{\overline{\beta^e}} = \nabla \wedge \overline{\overline{\beta^e}} \qquad (6.8)$$

It is essential to investigate what $\bar{\bar{\alpha}}$ represents. Applying Stoke's theorem to each component with the first index of $\bar{\bar{\alpha}}$:

$$\int\int_{\Sigma} \bar{\bar{\alpha}}\,\vec{dS} = \int\int_{\Sigma} \overrightarrow{rot}\,\bar{\bar{\beta}}\,\vec{dS} = \oint \bar{\bar{\beta}}\,\vec{dx} = \oint \vec{\beta}_j\, dx_j = \oint d\vec{u}^e$$

The flux of $\bar{\bar{\alpha}}$ through a surface S, defined by the closed path C, depends only on C. So let $\vec{b}$ the flux of $\bar{\bar{\alpha}}$ through S, as $\bar{\bar{\beta}}^e = \bar{\bar{\beta}} - \bar{\bar{\beta}}^p$ and $\overrightarrow{rot}\,\bar{\bar{\beta}} = 0$. We can then write:

$$b_i = \oint_C du_i^e = -\oint_C du_i^p = \int\int_S \alpha_{ij}\, dS_j \tag{6.9}$$

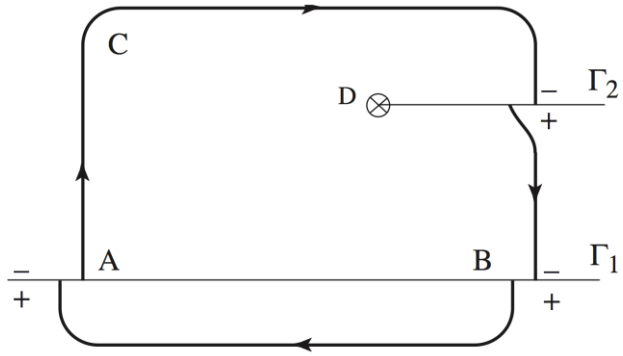

Suppose now that the circuit C crosses one of the surfaces where the plastic deformation has been introduced, i.e. cutting through the solid following the mentioned surfaces, then creating the displacement du_p of the edge + in relation to the edge -.

Following the definition of the vector of the circuit C points towards the positive edge (see Figure 6-10).

Figure 6-10: *Contour through the cutting surface*

For a cutting surface going through circuit C from part to part, the integral of $\vec{b}$ is zero because if we have du_i^p in A, it is $-du_i^p$ in B—only the cutting surfaces that stay within C count, their limit bound by the closed contour C. Let Γ_2 be a cutting surface attached by a curve D enclosed by the closed contour C; $\vec{b}$ becomes the displacement of the negative edge of Γ_1 to the positive edge of Γ_1. Γ_2 is oriented by C ($\vec{dl}$ being the positive normal vector to Γ). Consequently, curve D is equally oriented as the positive normal to the surface S, defined by path C (Figure 6-10). The curve D is called a dislocation line, $\vec{b}$ is the Burgers vector, and C is the Burgers circuit.

If the dislocations exist throughout the crystal, their density in a point M can be obtained by considering an infinitesimal circuit C serving as a contour for the infinitesimal surface ΔS centered at point M. We then have:

$$\alpha_{ij} = \frac{\Delta b_i}{\Delta S_j}$$

$\Delta\vec{b}$ represents the sum of the Burgers vectors of the dislocations encircled by C and $\bar{\bar{\alpha}}$ the tensor can be considered as the dislocation density in point M.

Remark: there exists a relationship with the theory of magnetic fields.

$$\vec{b} = \oint_C \overline{\overline{\beta^e}}\, d\vec{x}$$

We note that this expression is analogous to Ampère's theorem:

$$i = \oint_C \vec{H}\, d\vec{l}$$

We see that, despite one tensorial order difference, we can make the correspondence between:

$\vec{b} \leftrightarrow i$ from one side and
$\overline{\overline{\beta^e}} \leftrightarrow \vec{H}$ from the other

Transforming the contour integrals into integrals over the internal surface (Stokes' formula), we have:

$$\vec{b} = \oint_C \overline{\overline{\beta^e}}\, d\vec{x} = \int\int_S \overrightarrow{rot}\,\overline{\overline{\beta^e}} \cdot d\vec{S} = \int\int_S \overline{\overline{\alpha}} \cdot d\vec{S}$$

similar to

$$i = \oint_C \vec{H}\, d\vec{l} = \int\int_S \overrightarrow{rot}\vec{H} \cdot d\vec{S} = \int\int_S \vec{j} \cdot d\vec{S}$$

where $\overline{\overline{\alpha}} = \overrightarrow{rot}\,\overline{\overline{\beta^e}}$ is the dislocation density tensor, analogous to $\vec{j}$, the current intensity vector, which is equal to $\overrightarrow{rot}\vec{H}$. In the same way, as $\vec{j} = \overrightarrow{rot}\vec{H}$ induces $div\vec{j} = 0$, we have that $\overline{\overline{\alpha}} = \overrightarrow{rot}\,\overline{\overline{\beta^e}}$ implies $div\overline{\overline{\alpha}} = 0$, which means that a dislocation line as a current line cannot stop inside a solid. Therefore, closed dislocation (Burgers) circuits can only exist where the Burgers vector is conserved. In other words, the equation $div\overline{\overline{\alpha}} = 0$ means that the Burgers vector is conserved along a dislocation line, as for current density in a current line.

Thus, dislocation lines are the sources of internal stresses due to elastic incompatibilities, much like current lines are the sources of magnetic fields. While Ampère's microscopic model of current for magnetism is only helpful for calculations, in crystal plastic deformation, the dislocation lines created are actual physical entities that can be photographed. In this case, the Burgers vector is constrained to be a periodic multiple of the lattice to correspond to reasonable energies. Thus, these dislocations play an essential role in explaining the plastic behavior of crystalline solids.

d) Transposition of the crystal lattice

Plastic deformation can be conceptually thought of as resulting from the fact that certain parts of the crystal slide before others; gliding begins in a specific location and spreads progressively throughout the crystal. At a given instant, we can define a boundary between a part of the plane that has already slipped and the other still at rest (Figure 6-11). This boundary corresponds to a dislocation. The idea that deformation by gliding results from the movement of dislocations was introduced in 1934 by Taylor, Orowan, and Polanyi.

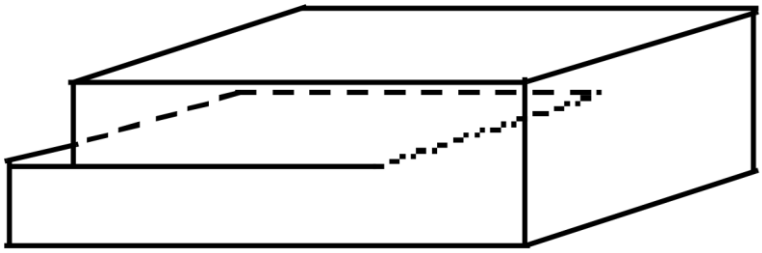

Figure 6-11: *Diagram of the localized gliding*

This assumption reminds us of what we previously explained in the theory of the incompatible elasticity framework. We showed that in the general case of deformation without fracture ($\overrightarrow{rot}\,\overline{\overline{\beta}} = 0$) and when the distribution of plastic deformations does not verify $\nabla \wedge \overline{\overline{\beta^p}} = 0$, an elastic deformation in the solid must exist such that $\overline{\overline{\alpha}} = \nabla \wedge \overline{\overline{\beta^e}} = -\nabla \wedge \overline{\overline{\beta^p}}$. In other words, the flux $\vec{b}$ of $\overline{\overline{\alpha}}$ through a surface S limited by the contour C, for a cutting surface Γ_2 (which stops at D inside the solid), leads to a discontinuity of the displacement,

$$\vec{b} = d\vec{u}^e = -d\vec{u}^p = \int\int_S \overline{\overline{\alpha}}\, d\vec{S}$$

where $\vec{b}$ is the displacement of the negative edge of Γ_2 relative to the positive edge of Γ_2 (Figure 6-10). Curve D delimiting the cutting surface Γ_2 enclosed by the contour C represents the boundary between the slipped part of the plane and the undeformed part. Figure 6-12 illustrates the transposition of Figure 6-8 in a crystal lattice.

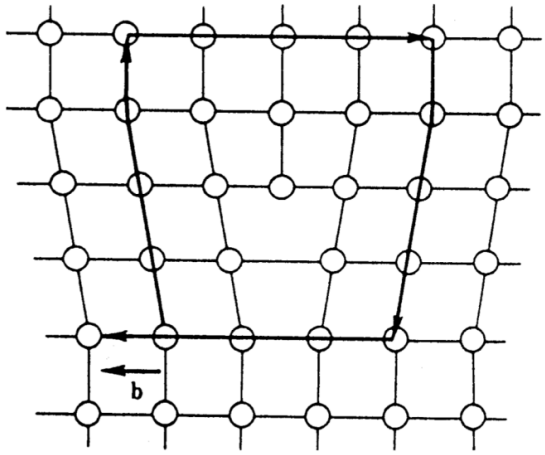

Figure 6-12: *Transposition of Figure 6-10 in a crystal lattice*

Slip, as it has been defined, requires only the motion of atoms in the vicinity of the boundary. The deformation is concentrated around the dislocation. It follows that it is sufficient to propagate the dislocation over a surface S for the crystal being sheared by $\vec{b}$ over this surface (Figure 6-13).

The atoms' displacements are no longer in phase, so the critical shear stress is expected to decrease considerably. We can **approximately say that a weaker force is at work over greater distances for the same amount of** work. If Λ is the distance covered by the dislocation motion ($\Lambda \approx \mu m$) instead of b ($\approx \mathring{A}$). We expect to have a reduction in the stress of the order of magnitude of

$$\frac{\Lambda}{b} \approx 10^4$$

If we suppose the equality in work holds in both cases. In fact, the (relative) disorder at the core of the dislocation helps the process even more. The stress required for dislocation propagation related to atomic motion is known as the Peierls-Nabarro stress.

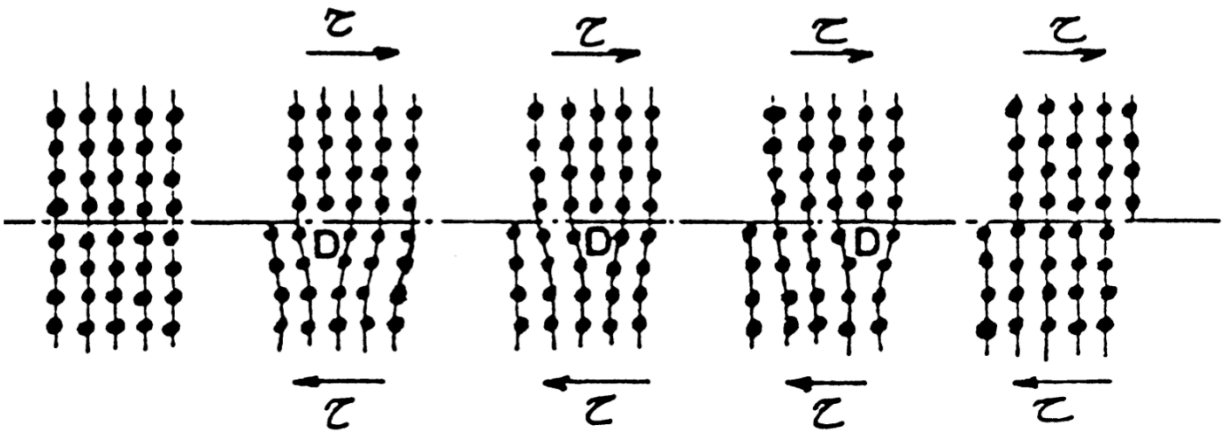

Figure 6-13: *Gliding of a dislocation in a crystal under the application of a shear stress τ*

6.2.3 Creation of a dislocation

a) In a continuous medium

The Creation of a dislocation line D in a continuous elastic medium requires the following operations (Figure 6-14):

1) The medium is cut following any surface S. The boundary between this surface and the rest of the medium is D.
2) The two edges, S_1 and S_2, are moved relative to each other without deformation. Here, only translational motions are considered, even though rotations could also be used.
3) We add or subtract matter so that when the operation is completed, there are no empty spaces or additional matter.
4) The matter is reattached along the surfaces, and the external stresses applied during these operations are relieved.

The dislocations hence created are called Volterra dislocations.

The dislocation line D forms a displacement field that varies from point to point in the medium, causing deformations and, consequently, stresses. Since the external surfaces are free, the stresses are zero. The internal stresses vary continuously in the crystal, even when crossing the surface S, assuming edges S_1 and S_2 do not deform (distort). Only a discontinuity in displacement exists going through S, while no discontinuity in deformation or stresses arises. The cutting surface has no physical meaning in the material; the result is the same regardless of the surface S chosen.

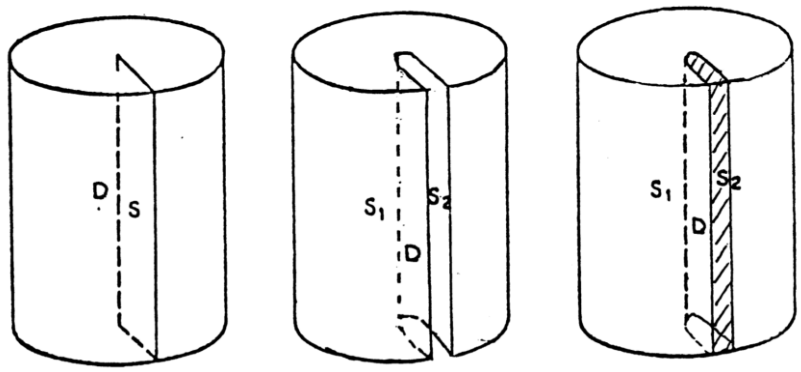

Figure 6-14: *Creation of a translational dislocation line in a continuous medium*

b) In a crystal lattice: Burgers vector

The above statements still hold their validity - except that displacement must now be equal to a shift corresponding to a lattice period such that the coupling does not depend on the choice of the cutting surface.
In this case, we use the Burgers vector and circuit notion to characterize the displacement. We define the Burgers vector $\vec{b}$ by the process suggested by Frank. But first, we consider a dislocation in a simple cubic structure.

Figure 6-15 shows a plane section of a cube with an edge dislocation. Again, we must distinguish the "perfect" crystalline regions, where the deformations are small, from the areas of "distorted" crystal, closer to the dislocation, where the deformations are significant.

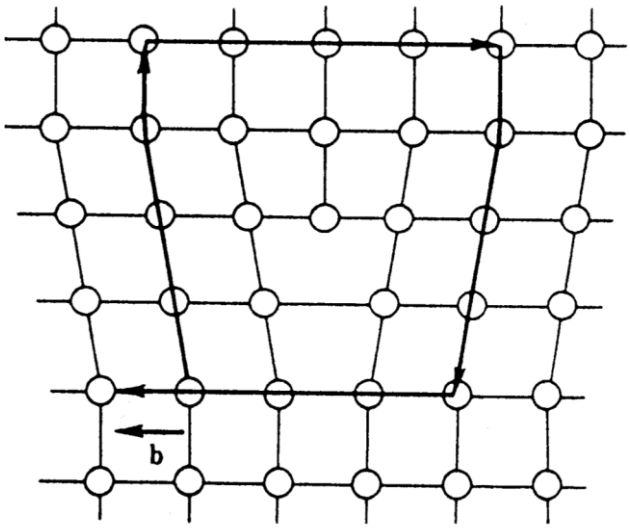

Figure 6-15: *Edge dislocation with its corresponding Burgers circuit*

To define the Burgers vector $\vec{b}$, we draw a closed contour around the dislocation line in the clockwise direction with the orientation of the dislocation line $\vec{\xi}$. This circuit is located within the "good" crystal that encircles the dislocation. Then, we draw the same circuit on the perfect crystal (Figure 6-16). The vector necessary to close the circuit is the Burgers vector $\vec{b}$ of the dislocation. Its direction

is from the final point to the initial point of the circuit. (This definition is not the only one in the scientific literature; many authors have given the opposite direction to the Burgers vector.)

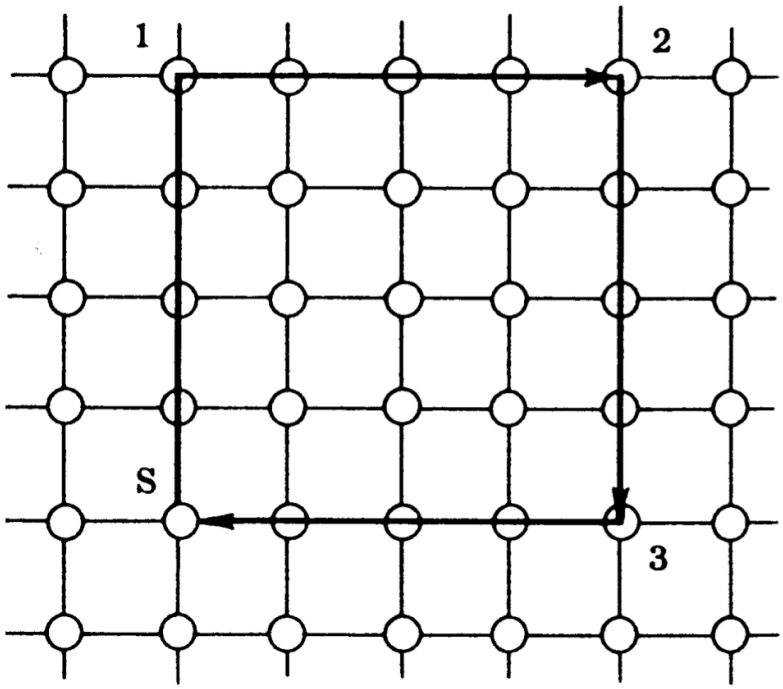

Figure 6-16: Burgers circuit in a perfect crystal

A dislocation is characterized by the following:

- the direction of its line $\vec{\xi}$
- its Burgers vector $\vec{b}$

and the angle ($\vec{\xi}$,$\vec{b}$) defines the type of dislocation (Figure 6-17).

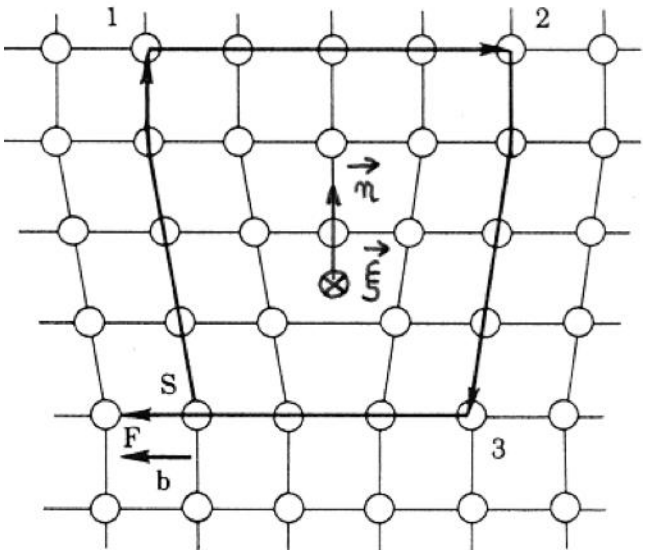

Figure 6-17: Burgers circuit in the deformed crystal

Remarks:

- Except for the cases where the Burgers vector $\vec{b}$ is parallel to the dislocation line $\vec{\xi}$, creating a dislocation line produces an extra half-plane, with one end coinciding with it (see Figure 6-17). The position of this additional half-plane can be obtained by considering the direct coordinate system ($\vec{\xi}, \vec{b}, \vec{n}$): $\vec{n}$ points in the direction of the plane. Conversely, if $\vec{\xi}$ and $\vec{n}$ are known, $\vec{b}$ can be obtained by completing the right-handed trihedron.
- Again, in the case where $\vec{b}$ and $\vec{\xi}$ are not parallel and for a conservative dislocation motion (i.e., without diffusion), the glide plane of the dislocation includes $\vec{b}$ and $\vec{\xi}$. Its normal is then defined by $\vec{\xi} \wedge \vec{b}$.
- There exists a specific terminology for the character of dislocations:
  - if $(\vec{\xi}, \vec{b}) = \pi/2$, we call it an edge dislocation (Figure 6-17)
  - if $(\vec{\xi}, \vec{b}) = 0$, we call it a screw dislocation (Figure 6-18), and it does not have a defined glide plane
  - mixed dislocation is the term used to indicate all other types of dislocations

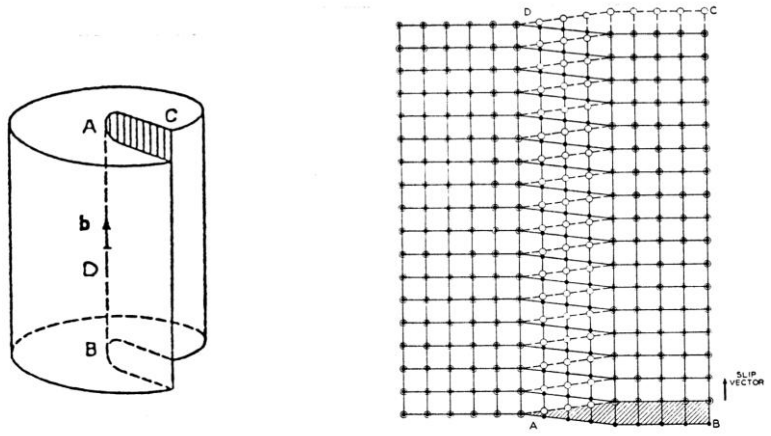

Figure 6-18: *Representation of a screw dislocation*

We note that the Burgers vector is perpendicular to the dislocation line in the case of an edge dislocation. For a screw dislocation, the vector $\vec{b}$ is parallel to the dislocation line (Figure 6-19).

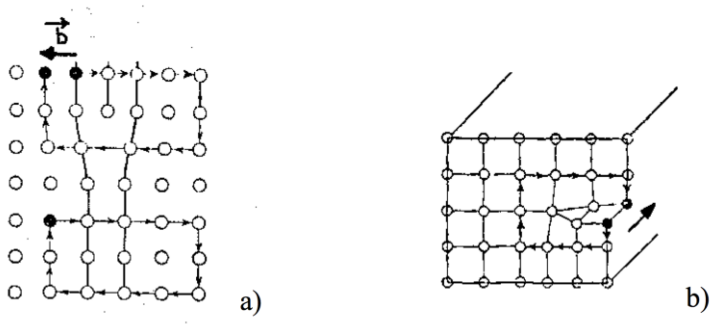

Figure 6-19: *Burgers vector for an edge dislocation (a) and a screw dislocation (b)*

6.3 General properties of dislocations

6.3.1 Dislocation loops

As noted earlier in the Chapter, dislocations cannot terminate within a crystal. Until now, dislocations have been described as emerging from both sides of the crystal on its surface. However, it is possible to imagine closed loops of dislocations inside the crystal. We consider two kinds of loops: glide loops and prismatic loops.

a) Glide loops

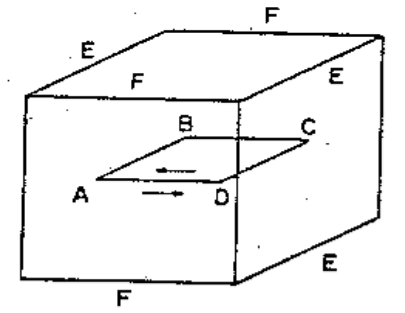

i) A cut is made following the ABCD plane. The atoms of the upper part are then displaced on the left by an interatomic distance. Let us consider what happens at the edges of the loop.

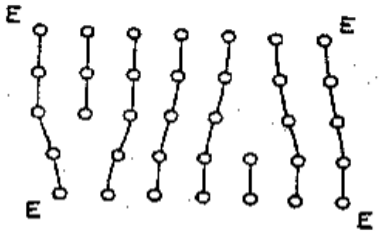

ii) We first observe what happens on AB and CD by making a section through EEEE. The displacement has introduced two edge dislocations of opposite signs. One of the segments has its extra half-plane pointing towards the upper part, the other towards the bottom.

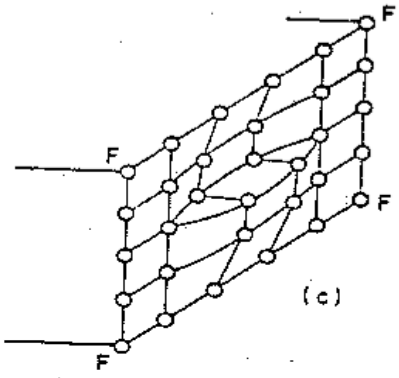

A section through FFFF shows screw dislocations. They must also be of opposite signs.

Figure 6-20: *Glide loop*

This dislocation line resides on dense atomic planes and could have any shape. Therefore, this loop configuration type is subdivided into portions of edge, screw, and mixed dislocations (Figure 6-21).

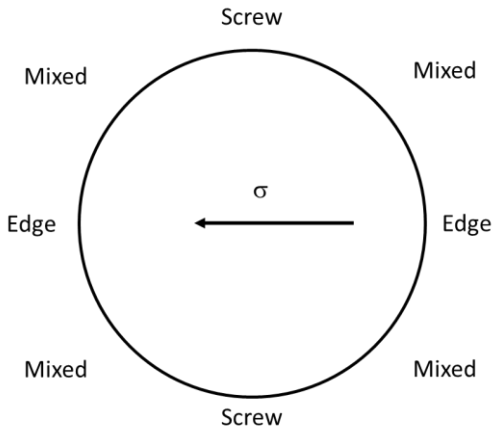

Figure 6-21: *Dislocation loop diagram*

b) Prismatic loops

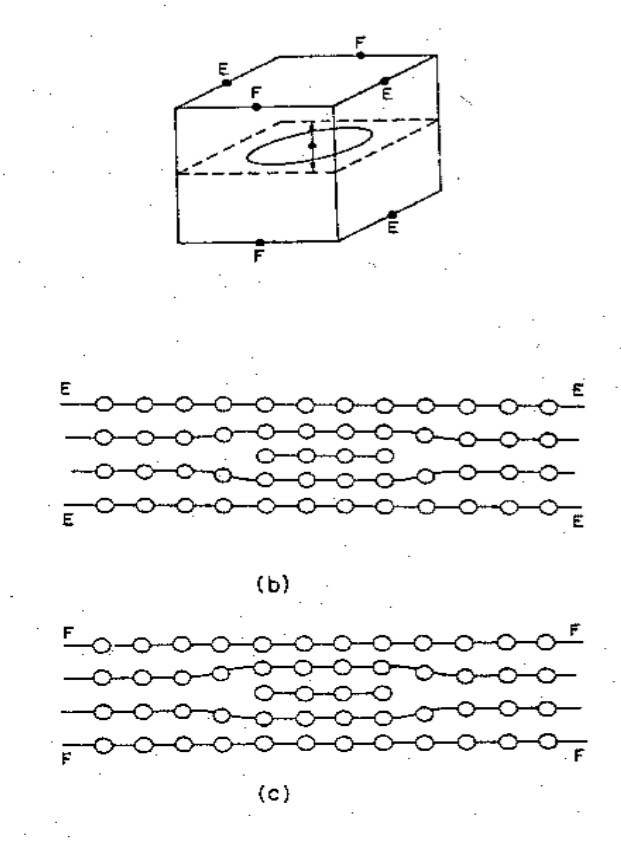

i) For the glide loops, we cut along a closed surface followed by a displacement in the plane where this surface lies. Here, we make the same cut, but instead of a parallel displacement, the two surfaces are separated by an interatomic distance, and the hole is filled with an extra plane.

ii) We note that the section EEEE:

(b) is identical to the FFFF section

(c) They both show edge dislocation. Instead of introducing an extra plane (interstitial loop), we could have removed one (vacancy-type dislocation loop), and the result would have been the same.

Figure 6-22: *Interstitial prismatic loop*

6.3.2 Properties of the Burgers Vector

Following the definition of the Burgers vector, we can list a few crucial properties.

• The vector $\vec{b}$ only depends on the nature of the "distorted" crystal encircled by the circuit. It does not rely on the shape or the origin of the circuit.
• For describing dislocations in terms of disconnections, the atomic displacement from one side of the disconnection is given by the Burgers vector $\vec{b}$. This vector expresses the crystal shear.

• We refer to a perfect dislocation as one surrounded by "perfect" crystal containing no defects. In this case, the vector $\vec{b}$ is a vector of the direct lattice.

• The displacement $\vec{b}$, which defines the dislocation line, has the same value all along the line. That is, the Burgers vector is conservative.

• If two dislocation lines, L1 and L2, end in the same line, L3, the Burgers vector of this dislocation is the sum of the other two vectors (Figure 6-23a). We then have:

$$\vec{b_3} = \vec{b_1} + \vec{b_2} \tag{6.10}$$

If we orient the lines towards the node of the dislocations, we have $\sum \vec{b_i} = 0$ (Figure 6-23b). This is equivalent to Kirchhoff's law in electricity. Thus, it is unsurprising to think of this analogy between $\vec{b}$ and $\vec{i}$ as discussed above.

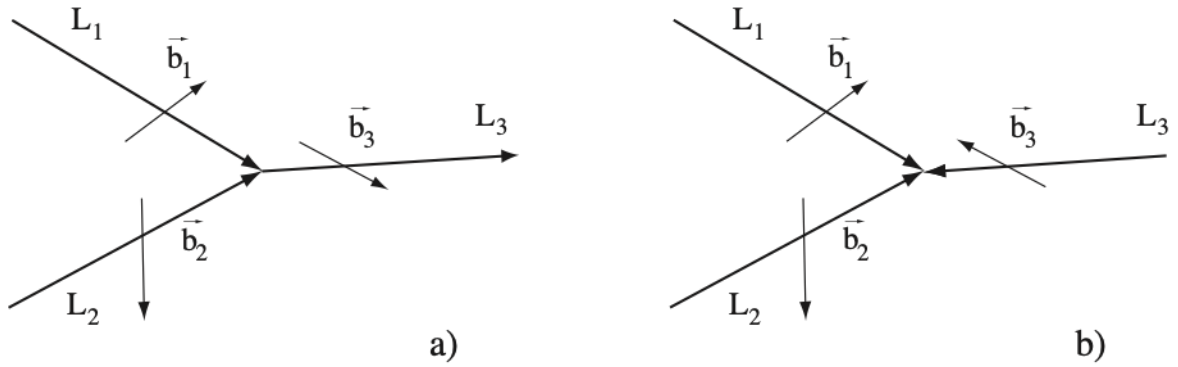

Figure 6-23: *Conservation of Burgers vector*

• If the Frank circuit encircles several dislocations (6-24), the Burgers vector of this circuit is the sum of the Burgers vectors of the dislocations contained in it.

• Figure 6-24: Frank circuit containing more than one dislocation $\vec{b} = \vec{b_1} + \vec{b_2} + \vec{b_3}$

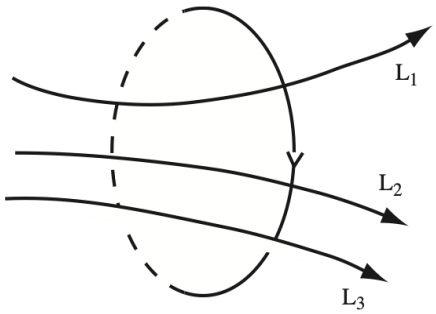

• For screw dislocations, $\vec{b}$ is parallel to $\vec{\xi}$; the dislocation is dextrorotatory if $\vec{\xi}$ and $\vec{b}$ are in the same direction ($\vec{\xi} \cdot \vec{b} = b$). It is levorotatory in the other case.

• In the case of a dislocation loop (glide loop), the $\vec{b}$ vector is constant, whereas $\vec{\xi}$ rotates by 2π. Therefore, the opposite sides of the loop have opposite $\vec{\xi}$ (Figure 6-25).

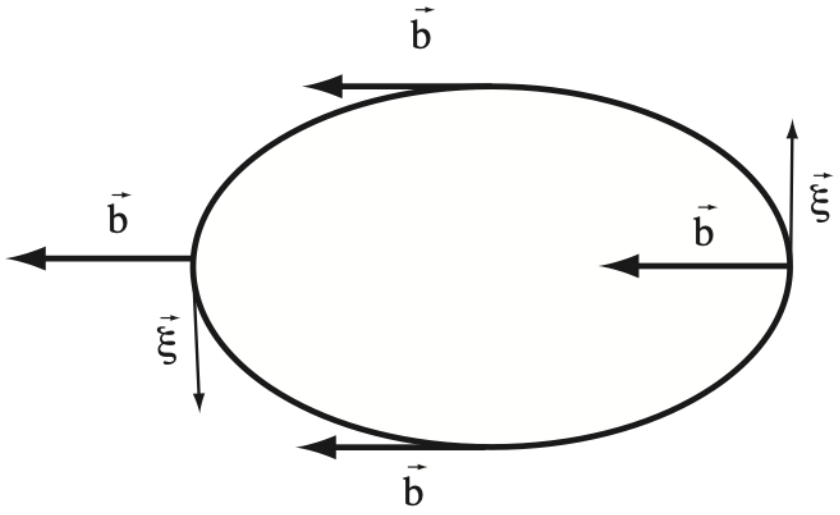

***Figure 6-25**: Glide loop: the Burgers vector is conserved*

6.4 Dislocation motion

When dislocations move, a crystal undergoes plastic deformation. Let us consider the case of a pair of edge dislocations of opposite signs (Figure 6-27). If stress is applied, these dislocations move in opposite directions. When dislocations move out of the crystal, an edge is created on both sides of the crystal. If the crystal contains several moving dislocations, we observe several "steps."

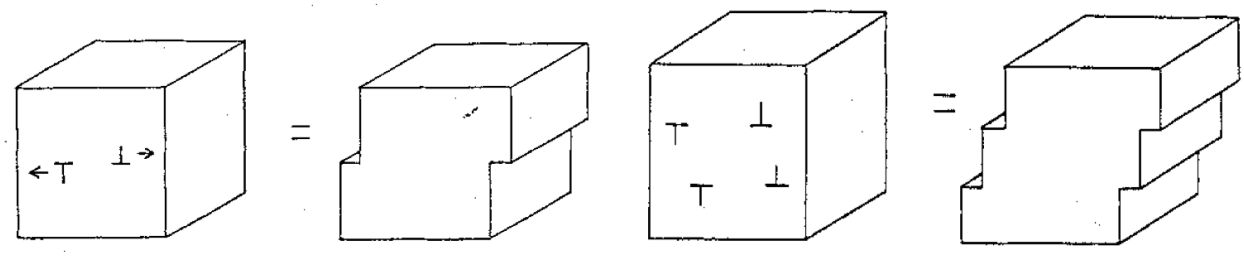

***Figure 6-27:** Edges showing up at the surface during the displacement of a pair of edge dislocations*

We note that the result is as expected for the displacement of one plane by an interatomic distance to the other. The motion of a screw dislocation is somewhat more complex to grasp.

We understand from Figure 6-20 that when a shear stress τ is applied, the two points A and B tend to separate, and the two screw dislocations. When dislocations reach the surface, they produce two "steps" (Figure 6-28). The displacement of the screw dislocation is perpendicular to the displacement of the atoms, that is, perpendicular to the stress.

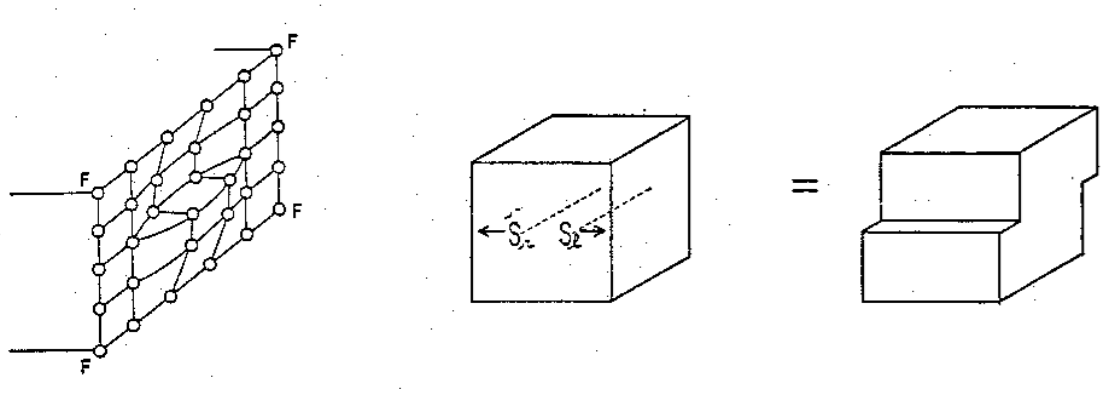

Figure 6-28: *Step" edges appearing on the surface during the displacement of a pair of screw dislocations*

From the combined motions of screw and edge dislocations that we discussed, it is easy to understand what happens in the case of a glide loop (see Figure 6-29).

When the loop has come out of the crystal, we have the same result as if:

i) An edge dislocation had crossed the entire crystal.

ii) A screw dislocation had crossed the entire crystal.

iii) A pair of edge dislocations had gone out of the crystal.

iv) A pair of screw dislocations had exited the crystal.

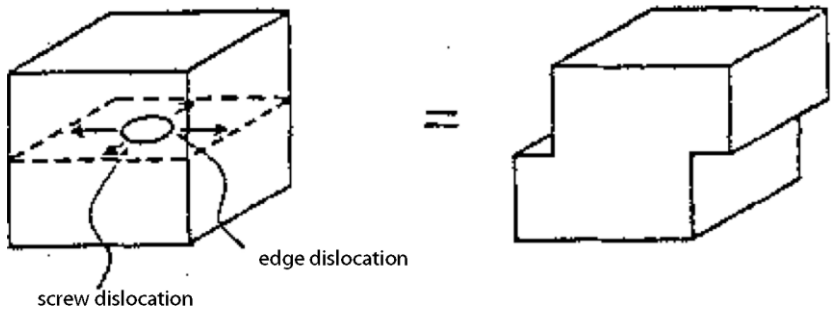

Figure 6-29: *Step" edges appearing on the surface during the displacement of a dislocation loop*

6.4.1 Glide plane

We note that a dislocation can only move without mass transfer (conservative motion) in the plane defined by the vectors $\vec{\xi}$ and $\vec{b}$. This plane is referred to as the glide plane of the dislocation.

Screw dislocations do not have a well-defined glide plane ($\vec{\xi}$ and $\vec{b}$ are parallel) but generally move in a densely packed lattice plane. (e.g., (111) planes in f.c.c.). During their displacement, they can change the glide plane (for example, they can vary from a (111) plane to a $(1\bar{1}1)$ plane if their Burgers vector is in the [111] direction); this behavior is referred to as "cross-slip." This dislocation motion can make it possible to dodge some obstacles; in Figure 6-30, we can observe the double cross-slip of a dislocation loop with Burgers vector. $\vec{b} = \frac{a}{2}[\bar{1}01]$

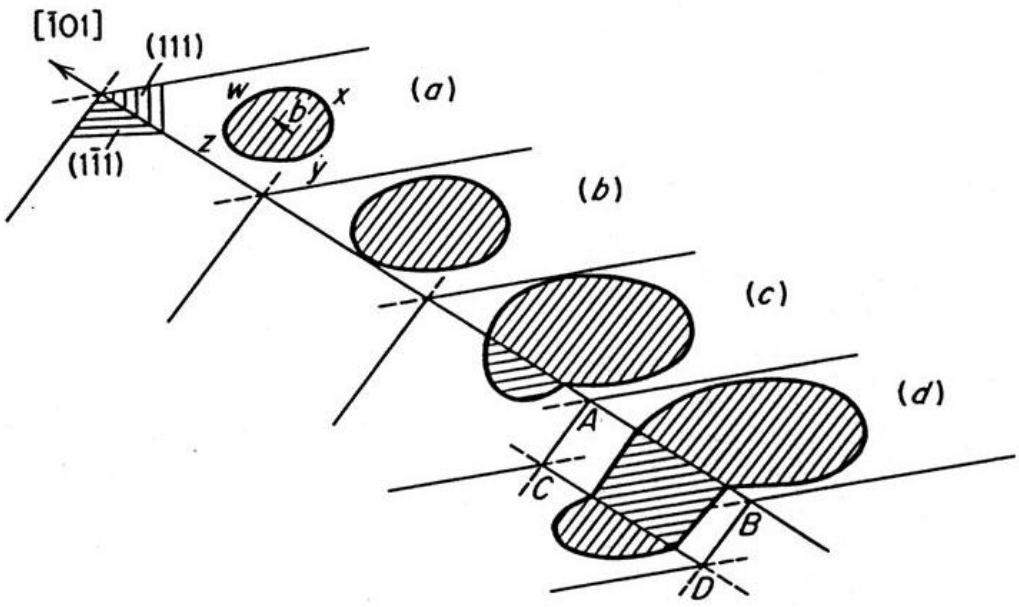

Figure 6-30: *The cross-slip of a dislocation loop*

6.4.2 Climb of a dislocation

As we discussed, the motion of a dislocation in its glide plane is a phenomenon that occurs without mass transfer. This is not the case for an edge or mixed dislocation moving perpendicularly to this glide plane.
For an edge dislocation to move (climb) by an interatomic distance perpendicular to its glide plane (vertical motion shown in Figure 6-31), a row of atoms must be removed or brought with the dislocation line. This mechanism can only happen by mass diffusion. In the case shown in Figure 6-31, the upward dislocation motion can only be accomplished by diffusion of vacancies towards the dislocation. The Creation of vacancies accompanies a downward dislocation motion. We note that dislocations can be sinks or sources of vacancy defects (or interstitials). Since the dislocation climb requires the formation and migration of point defects, it can only happen at reasonable speeds at high temperatures when thermally activated.

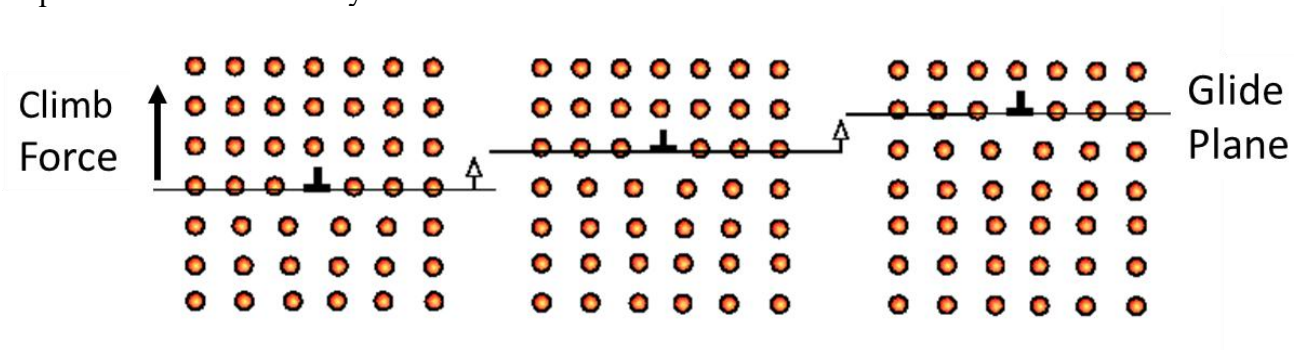

Figure 6-31: *Climb of dislocation to a vacancy line*

For prismatic loops that cannot move along their glide cylinder, a motion in the plane of the loops occurs that conserves the size of these loops. It is neither a gliding process nor a climb mechanism, as there is no mass diffusion toward the loops. The mechanism can only be produced by the diffusion of vacancies (or interstitials) along the dislocation line (pipe diffusion), referred to as conservative climb.

6.4.3 Relation between dislocation motion and plastic deformation

We have observed that the movement of dislocations involves a plastic deformation; it must be possible to establish a relation between this motion and the deformation caused by it. Consider first the case in which a crystal in the shape of a parallelepiped (L1 L2 L3) (Figure 6-32) is crossed by a straight edge dislocation with Burgers vector $\vec{b}$,

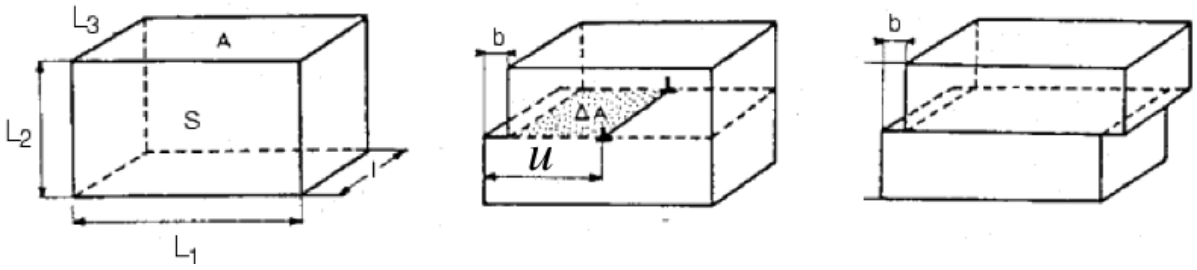

Figure 6-32: *Deformation resulting from the gliding of a dislocation*

When the dislocation has crossed the whole crystal, it has caused a plastic deformation ε given by:

$$\varepsilon = \frac{b}{L_2}$$

If the dislocation only moves by a distance *u*, the deformation can be given by

$$\varepsilon = \frac{b}{L_2}\cdot\frac{u}{L_1} = \frac{b}{S}u \qquad S = L_1 L_2 \tag{6.11}$$

or if it is displaced over the surface $\Delta A = u \cdot L_3$, then:

$$\varepsilon = \frac{b}{L_2}\frac{\Delta A}{L_1 L_3} = \frac{b}{V}\cdot\Delta A \qquad V = L_1 L_2 L_3 \tag{6.12}$$

If we now suppose that N_m parallel dislocations have moved in this same glide plane or others parallel to it, the deformation after they have all crossed an equal area ΔA is given by:

$$\varepsilon = \frac{N_m}{V}\cdot b\Delta A \tag{6.13}$$

where $$\varepsilon = \frac{N_m}{S} bu \tag{6.14}$$

We introduce then the notion of the density of mobile dislocations in their glide planes Λ_m defined by:

$$\Lambda_m = \frac{N_m}{S} = \frac{N_m \cdot L_3}{V} \tag{6.15}$$

We notice that this quantity expresses:

- either the average number of dislocations emerging per unit surface
- or the total length of the dislocations per unit volume

We then have:

$$\varepsilon = \Lambda_m b \cdot u \tag{6.16}$$

If we also assume that every dislocation moves with the same speed, we can express the deformation speed by:

$$\dot{\varepsilon} = \Lambda b \dot{u} = \Lambda b v \tag{6.17}$$

It is Orowan's equation. This is one of the most important equations and concepts of this course.

Thus, we notice that the plastic deformation velocity is directly linked to the speed of the dislocations. Therefore, the dislocations appear as the "carriers" of plastic deformation, in the same way as electrons are for electric current.

6.5 Multiplication of dislocations

6.5.1 Hardening phenomenon

Direct observations of dislocations, such as those made using electron microscopes (Figure 6-33), clearly show that the increase in dislocation density accompanies plastic deformation. Dislocation densities vary from $\Lambda = 10^6$ cm^{-2} to $\Lambda = 10^{11}$ or 10^{12} cm^{-2} after plastic deformation in metals. We know from experience that metals become harder during the deformation process. For instance, in Figure 6-34, we observe an increase in the yield strength ($\tau_2 > \tau_1$) during repeated loading/unloading cycles. This effect is caused by the "tangling" of dislocations, which mutually interfere with their motion and hence cause the "work hardening" and a substantial increase in internal stresses. Fracture occurs when the plastic deformation is made impossible by the dislocations completely blocking each other out (point R in Figure 6-34).

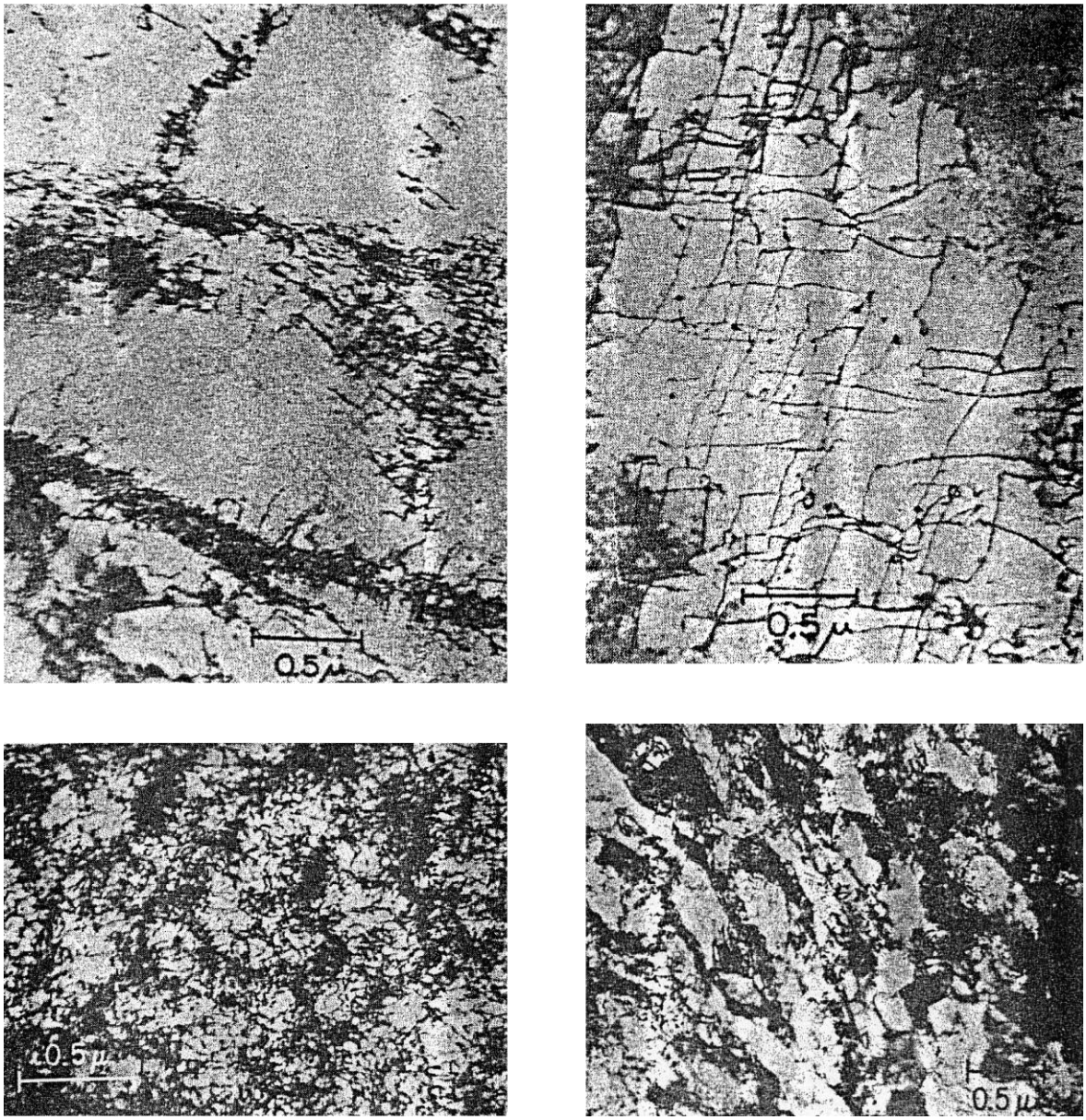

Figure 6-33: *Arrangement of dislocations produced by plastic deformation of iron at 20˚C (deformed to 9%) [top left]; at -135˚C (deformed to 7%) [top right]; Arrangement of dislocations in an iron-silicon alloy deformed at 20˚C [bottom left] and deformed to 20% and annealed 15 min at 600˚C [bottom right].*

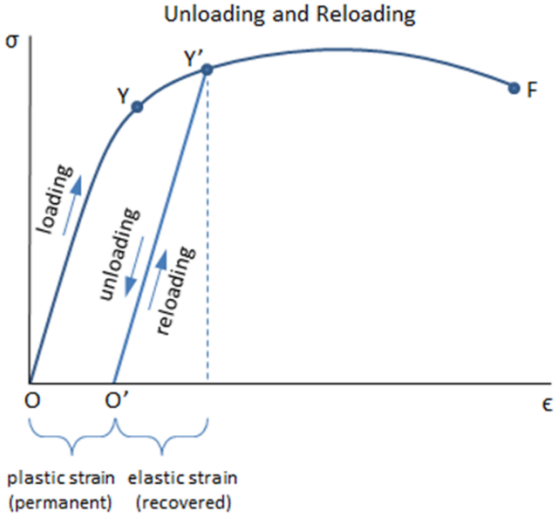

Figure 6-34: *Increase in the yield strength during consecutive loadings of a sample*

6.5.2 Sources of Dislocations

The increase in dislocation density during plastic deformation provides evidence that there must be sources of dislocations. Several mechanisms have been suggested; the simplest one is the one conceived by Frank and Read (Figure 6-35).

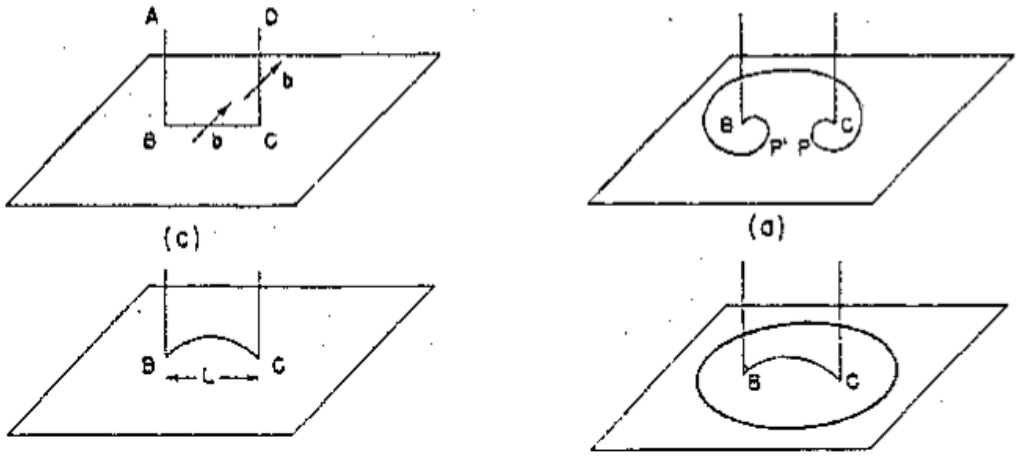

Figure 6-35: *Formation of a dislocation loop by the Frank-Read mechanism*

Consider a dislocation line ABCD, with only the segment BC situated in a glide plane: B and C are thus anchor points. When a shear stress τ is applied, the segment BC bows into an arch shape. For $\tau > \tau_{crit}$, the loop extends until the two segments, P' and P, touch. Since these two loop segments have line vectors of opposite signs but equal length, they cancel out (**remember Burger's vector is conversed quantity!**). What remains is a glide loop, which continues to grow, and a new arch forms, continuing the process to radiate dislocation loops. It is a Frank-Read source.

6.5.3 Other hardening processes

The motion of dislocations is perturbed by the presence of other dislocations (work hardening); we can also block the dislocations by introducing other atoms in the lattice (interstitial and substitutional impurities, precipitates).

a) Pinning of dislocations

Very often, interstitial impurities (C, N, O) diffuse towards the dislocations and make their motion very hard; this phenomenon corresponds to an increase in the yield strength of the material.

For example, the tensile stress-strain curve of iron and mild steel (Figure 6-36) exhibits a distinctive aspect of these materials: a higher yield point followed by a drop in stress, known as the lower yield point, at which the material deforms at a constant stress value. To understand this phenomenon, we assume that impurities block dislocations. Then, under applied stress, dislocations are progressively "unblocked" from their cloud of impurities and move. As a result, the activation and propagation of series dislocations in a common glide plane can develop macroscopic slip bands called Lüders bands. This phenomenon always appears after aging, during which other atoms can migrate towards the dislocations, and is not observed just after a slight deformation - in other words, after the Creation of new dislocations.

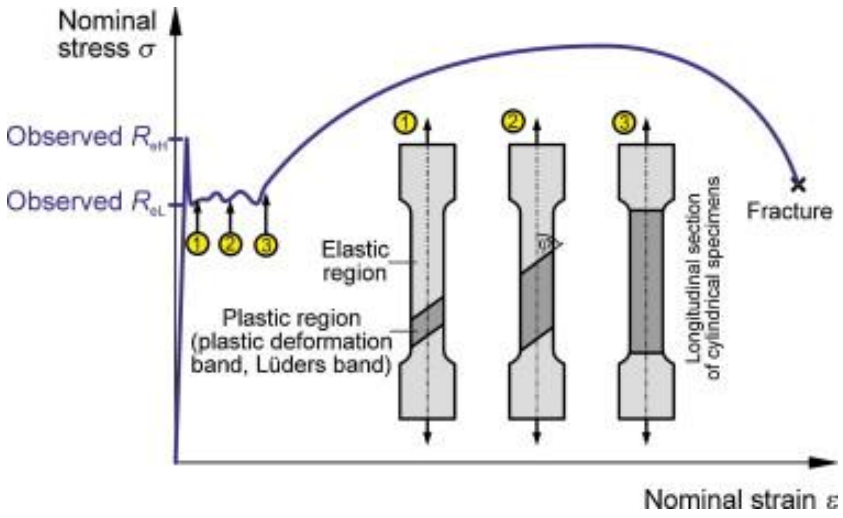

Figure 6-36: *Characteristic stress-strain curve for mild steel*

b) Structural hardening

The elements of an alloy, in solid solution or as dispersed phases, modify the plastic properties of the base metal. Figure 6-37 shows the effect of some thermal processes on an Al-2% alloy. After quenching, we have an oversaturated solid solution of Cu in aluminum. The following thermal processes cause the precipitation of copper as small particles with different characteristics (size, coherence with the matrix).

These age-hardening processes are accompanied by a substantial variation in the mechanical properties of the alloy as well. These processes can be described as the interaction between dislocations and obstacles that impede their motion. Here, these obstacles are precipitates.

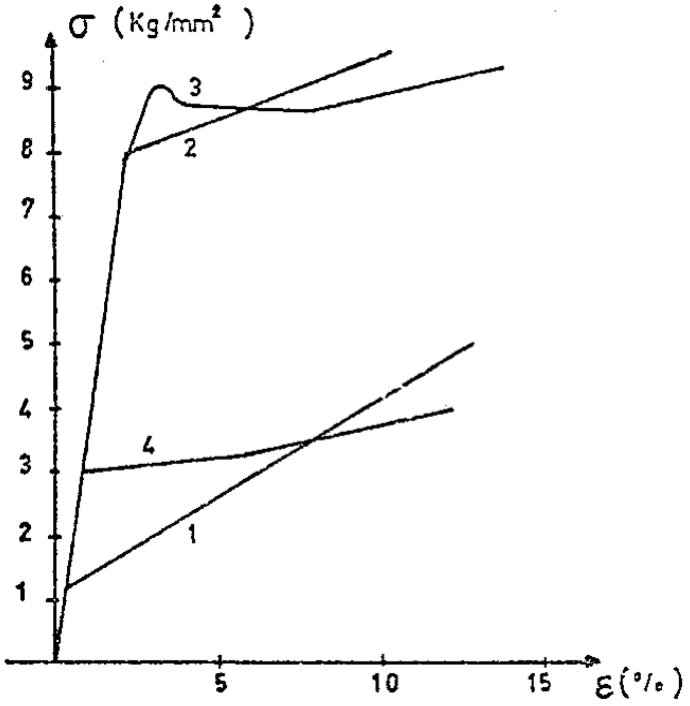

1. *Aged for 2 days at 350˚C, the metal contains incoherent particles: small CuAl3 rods 2.5µm distant.*
2. *Aged for 27.5 hours at 190˚C, the metal contains incoherent particles at 400 Angstrom distance.*
3. *Aged 2 days at 130˚C, the metal contains Guinier-Preston zones (very thin zones of 100 Å of diameter and atomic planes situated 150 Å distant.*
4. *Simply quenched, the metal is a solid solution.*

Figure 6-37: *Effect of different thermal treatments on the deformation of an alloy Al-2%-Cu. Measurements were taken at -196˚C.*

6.6 Recrystallization

In this Chapter, we showed how the deformation of the material causes a significant increase in the concentration of dislocations (Λ increases from 10^6 to 10^{11} cm^{-2}). This phenomenon corresponds to a substantial increase in internal energy. For the crystal to return to its initial state, it must eliminate the dislocations generated by plastic deformation. Recrystallization is often the primary mechanism associated with the full recovery of dislocations. This recovery is the thermodynamic driving force of recrystallization.

Figure 6-38 a)-h) shows the recrystallization and rapid grain growth resulting from the stored energy of dislocations in a heavily deformed gold polycrystalline sample. Recovery and annihilation of dislocations drive recrystallization, which causes a reduction of residual stresses, dislocation density, and internal energy (Figure 6-38: i). Grain growth requires the diffusion of atoms through the interface. It can only be achieved at high temperatures, so the full recovery of metals can only be performed at high temperatures.

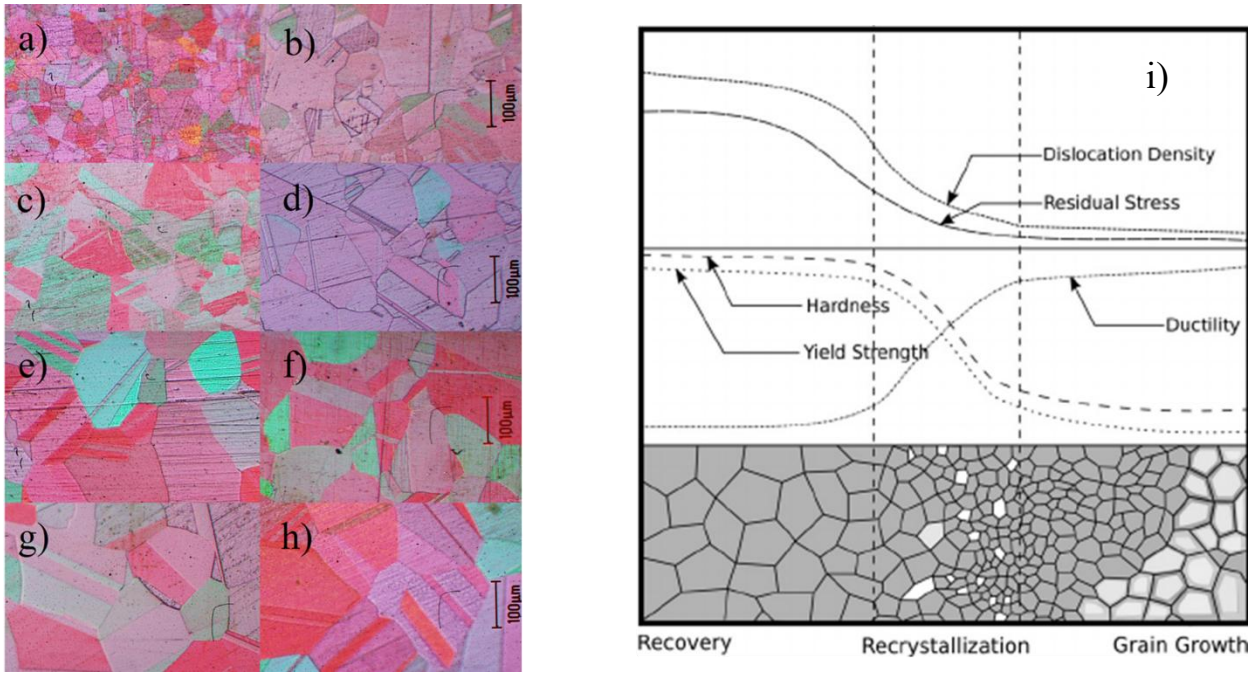

Figure 6-38: *The recrystallized grain (arrow) does not contain dislocations anymore*

6.7 Crystal growth

The presence of dislocations is a necessary condition for crystal growth. We consider the crystal growth starting from a lightly oversaturated vapor phase. The growth is caused by the deposition of atoms on the surface. In principle, this surface is not regular but shows incomplete layers of atoms bounded by *steps*. These steps are not necessarily straight but can exhibit edges called *jogs* (Figure 6-39).

Consider the effect of vapor pressure. Some atoms in the vapor are absorbed on the surface. Only surface diffusion is fast enough for the absorbed atoms to diffuse over a long distance until they reach a step. Then, atoms diffuse along the step until they reach a jog. Since they are in contact with the crystal on 3 of the six faces, atoms are bound more strongly. We can then say there is equilibrium when atoms join and leave the jog with the same frequency.

On the other hand, if there is a light oversaturation, more atoms join the jog than leave; the step "climbs" up until it reaches the edge of the crystal. Then, we can observe the layers fill progressively, and the steps disappear. New layers must nucleate to continue the growth. The presence of a nucleus (an isolated monolayer) increases the surface energy, and this nucleus is not stable unless it reaches a specific critical size. The probability that a nucleus with the required size is formed depends heavily on the oversaturation. An oversaturation of 25% to 40% is necessary for growth to occur at a noticeable speed.

In contrast to the previous predictions, the speed of crystal growth increases almost proportionally to oversaturation for small values, ranging from 3% to 4% (Figure 6-40). The curve found experimentally is produced if the formation is unnecessary and steps already exist on the surface. To explain this phenomenon, Frank supposed that the growing crystal was not perfect but contained screw dislocations.

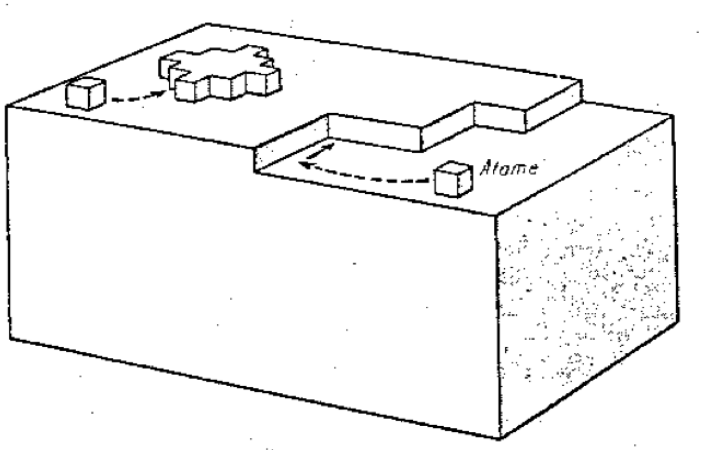

Figure 6-39: *Growth by sublimation*

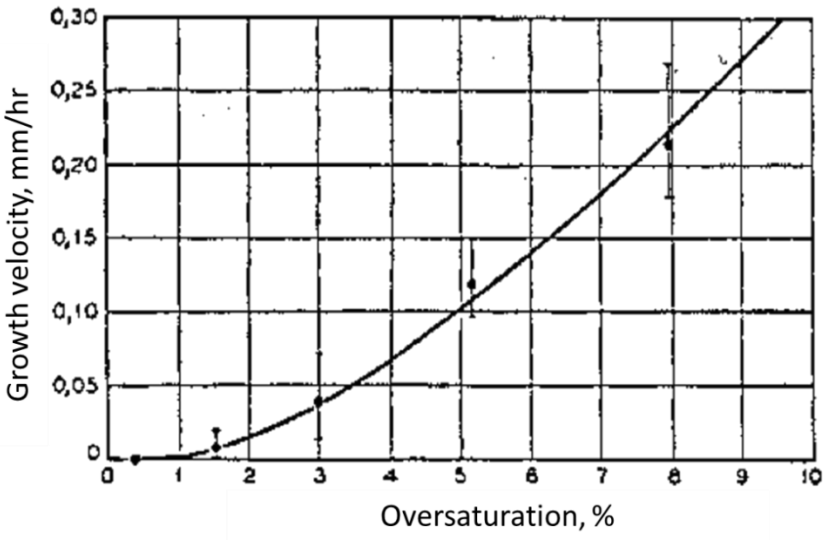

Figure 6-40: *Growth speed of a monocrystal as a function of the oversaturation of the atmosphere*

Figure 6-41 illustrates Frank's explanation: a screw dislocation reaches the surface of the crystal, normal to it, creating a step from the end of the dislocation to the edge of the crystal. When the surface

absorbs atoms, they diffuse towards this step, which then moves sideways. However, this motion cannot complete a uniform atomic layer because the upper surface is a spiral ramp.

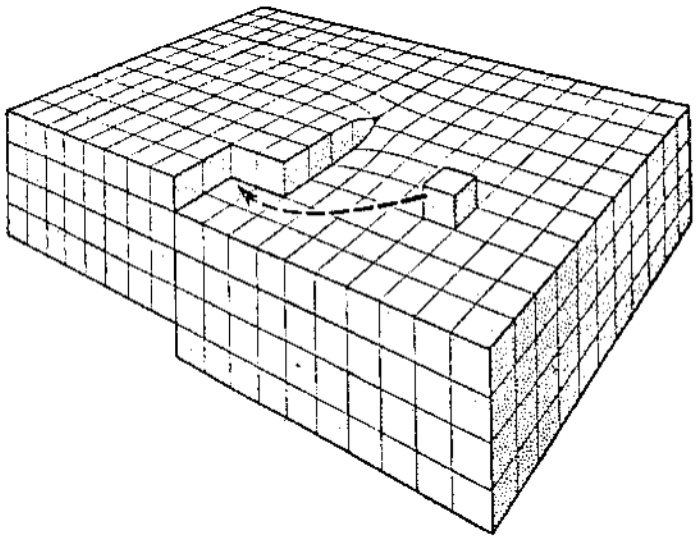

Figure 6-41: *Growth on the front of a screw dislocation*

We can easily understand (Figure 6-42) that during the growth, the step moves as a rigid spiral that rotates around its center O with a certain angular velocity ω

$$\rho = 2\rho_c\theta \qquad \text{and} \qquad \omega = \frac{d}{dt}\left(\frac{\rho_\infty}{2\rho_c}\right) = \frac{v_\infty}{2\rho_c}$$

$2\rho_c$ = critical radius of the nucleus previously mentioned

v_∞ = sideways displacement speed of a step with infinite radius (straight step)

ρ = instantaneous radius of the spiral

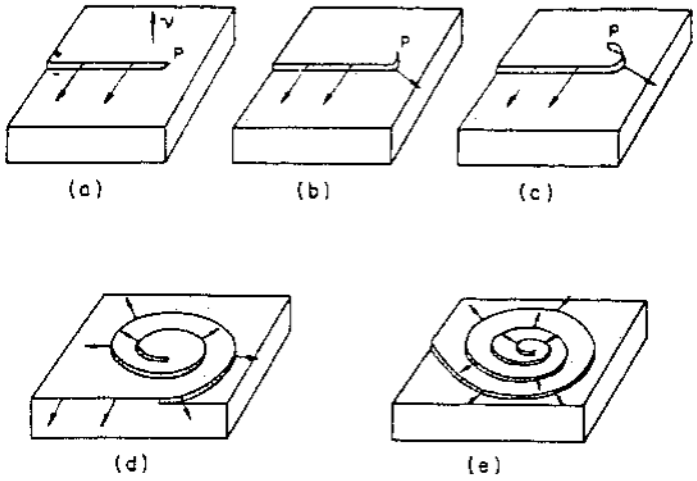

Figure 6-42: *Diagram of the spiral growth on a screw dislocation*

Figure 6-43 shows the result obtained on the face c of a "salol" crystal made from a solid solution of carbon bisulfide. Figures 6-43 b) and c) represent the growth spirals obtained on the base plane of silicon carbide.

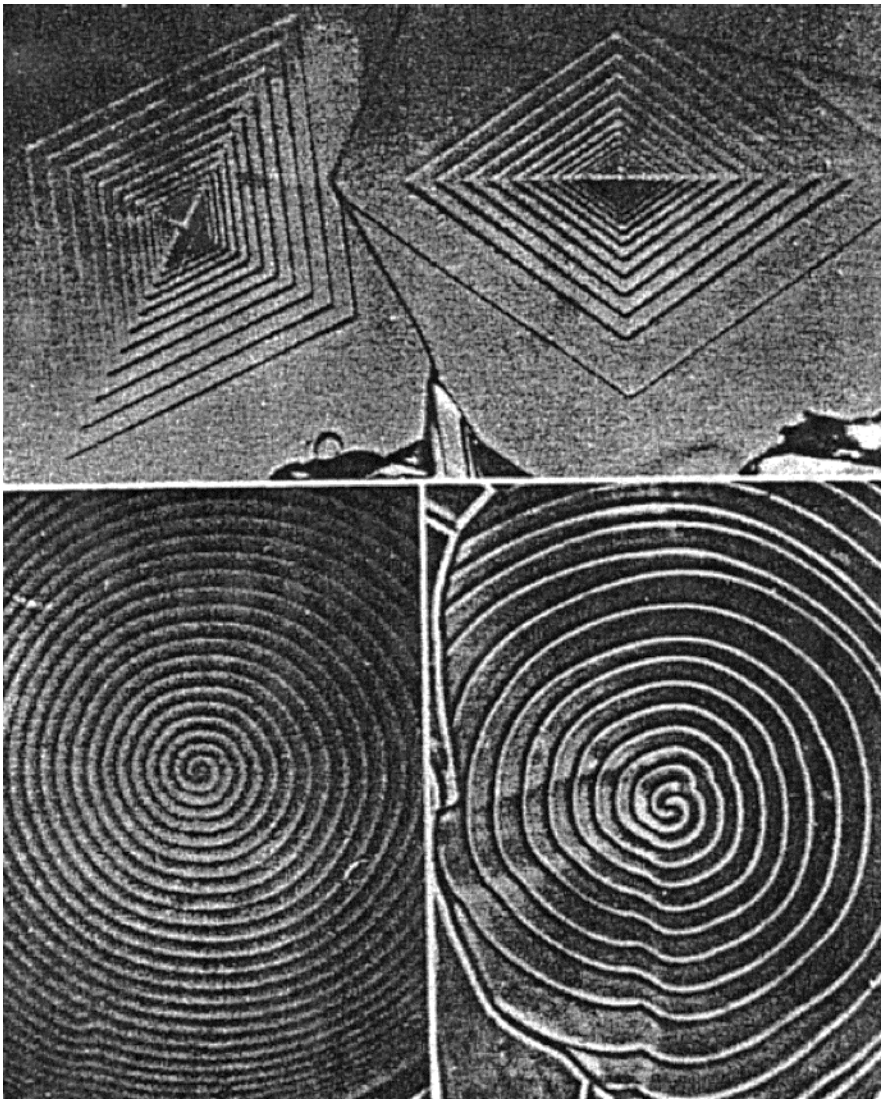

Figure 6-43: *Images illustrating the growth stimulated by the presence of a screw dislocation. a) The surface of a polyethylene crystal. b) and c) SiC crystal.*